AgriEngineering

MDPI

Article

Performance of Vegetation Indices to Estimate Green Biomass Accumulation in Common Bean

Thiago Orlando Costa Barboza *, Matheus Ardigueri, Guillerme Fernandes Castro Souza, Marcelo Araújo Junqueira Ferraz, Josias Reis Flausino Gaudencio and Adão Felipe dos Santos

Department of Agriculture, School of Agricultural Sciences of Lavras, Federal University of Lavras (UFLA), Lavras 37200-900, Brazil; adao.felipe@ufla.br (A.F.d.S.)

* Correspondence: thiago.barboza@estudante.ufla.br

Abstract: Remote sensing technology applied to agricultural crops has emerged as an efficient tool to speed up the data acquisition process in decision-making. In this study, we aimed to evaluate the performance of the Normalized Difference Vegetation Index (NDVI) and the Normalized Difference Red Edge (NDRE) in estimating biomass accumulation in common bean crops. The research was conducted at the Federal University of Lavras, where the ANFC 9 cultivar was used in an area of approximately seven hectares, in a second crop, in 2022. A total of 31 georeferenced points spaced at 50 m were chosen to evaluate height, width and green biomass, with collections on days 15, 27, 36, 58, 62 and 76 of the crop cycle. The images used in the study were obtained from the PlanetScope CubeSat satellite, with a spatial resolution of 3 m. The data obtained were subjected to a Pearson correlation (R) test and multiple linear regression analysis. The green biomass variable was significantly correlated with plant height and width. The NDVI performed better than the NDRE, with higher values observed at 62 Days After Sowing (DAS). The model that integrates the parameters of height, width and NDVI was the one that presented the best estimate for green biomass in the common bean crop. The M1 model showed the best performance to estimate green biomass during the initial stage of the crop, at 15, 27 and 36 DAS (R^2 = 0.93). These results suggest that remote sensing technology can be effectively applied to assess biomass accumulation in common bean crops and provide accurate data for decision-makers.

Keywords: remote sensing; NDVI; NDRE; *Phaseolus vulgaris* L.; monitoring

Citation: Barboza, T.O.C.; Ardigueri, M.; Souza, G.F.C.; Ferraz, M.A.J.; Gaudencio, J.R.F.; Santos, A.F.d. Performance of Vegetation Indices to Estimate Green Biomass Accumulation in Common Bean. *AgriEngineering* **2023**, *5*, 840–854. https://doi.org/10.3390/agriengineering5020052

Academic Editor: Mathew G. Pelletier

Received: 6 March 2023
Revised: 1 May 2023
Accepted: 3 May 2023
Published: 4 May 2023

1. Introduction

Common bean (*Phaseolus vulgaros* L.) is an important component of the Brazilian diet due to its high protein value [1]. Its per capita consumption in natura is 16 kg:person^{-1} year^{-1} [2]. Given its economic and social importance, as well as the high variability in productivity across the national territory, it is relevant to develop techniques and methods that enable the monitoring of plant morphological changes in bean crops.

Biomass production evaluations are important because these variables are directly correlated with crop gain productivity [3]. However, in many agricultural crops, biomass quantification follows the direct sampling protocol, which requires representative sample areas and is highly costly.

In this scenario, the development of technologies that aid in obtaining information in a non-destructive and sustainable manner is important [4]. Remote sensing is a technology that allows monitoring the crop cycles, acquiring information related to physical and biological characteristics of the crop [5]. Several techniques seek to establish relationships between the radiation absorbed by the crop canopy and the biophysical attributes. In healthy plants, adequately supplied with water and nutrients, there is a positive linear relationship between the amount of photosynthetically absorbed radiation by the canopy and biomass production [6].

Vegetation indices (VI) have been widely used due to their ability to predict and evaluate characteristics of vegetation cover, such as leaf area estimation, biomass production, and productivity [7–10]. Such information can be a valuable tool for producers and research institutions, as it is useful in decision-making, crop management, harvest planning, crop yield forecasting, information gathering and monitoring.

These VIs enhance the spectral interaction of plants and correlate with biophysical parameters of vegetation, such as canopy biomass. According to [11], the performance of vegetation indices, including the Normalized Difference Vegetation Index (NDVI), was evaluated in wheat crops by correlating them with biophysical parameters, and NDVI showed better correspondence with biomass. It was also used for estimating total eucalyptus biomass at local and regional scales through the NDVI, Soil-Adjusted Vegetation Index (SAVI), Simple Ratio (SR) and Enhanced Vegetation Index (EVI) [12]. Furthermore, there is a strong correlation between vegetation biomass and data obtained by orbital remote sensing [6].

Biomass is an inherent characteristic of the growth and development process of crops, which correlates with VI. Many authors used VI to estimate the biomass. In pasture, seven VI, used to estimate the biomass, and the NDVI showed a good relationship described by the accuracy and precision of the models [13], the soybean biomass estimate showed a strong correlation with the VI in Brazil [14], and in corn with the use of VI it was possible to estimate the biomass 77 days after sowing of the irrigated plants [15].

There are few studies that used vegetation indices to estimate the biomass for the common bean. With these VI, it is possible to perform temporal and spatial monitoring of the development of the bean crop, estimate canopy biomass and make future harvest predictions [3]. Thus, this article will help open new ways to use VI to improve the management of crops, help farmers in increasing production and promote the production of this plant.

Some studies involving the evaluation of biomass production of bean cultivar, as well as the use of remote sensing techniques, become important in assessing the potential of these methods for biomass estimation. Thus, the objective was to evaluate the performance of NDVI and the Normalized Difference Red-Edge index (NDRE) in estimating green biomass of the bean crop through vegetation indices. The remainder of this paper is divided as follows: Section 2 describes the project development; Section 3 presents the results obtained with the research, the importance of using the VI and its correlation with the biomass of common bean plants; finally, conclusions are presented Section 4.

2. Materials and Methods

The study was developed in a commercial area located in the state of Minas Gerais, in the city of Ijaci. The property belongs to the Federal University of Lavras (UFLA), known as the Scientific and Technology development center—Fazenda Muquém. The climate in the municipality is Cwa [16], temperate and rainy, with dry winters and rainy summers, and the temperatures of the warmest month are greater than 22 °C [17].

In the study area, on 18 February 2022 (second harvest), we carried out the sowing of a short-cycle cultivar of carioca beans (ANFC 9), with a growth period of 88 to 90 days and upright stature. We adopted a spacing of 0.6 m between rows and 250,000 plants sowed per hectare, and a seed fertilization of 250 kg/ha of NPK 08-28-16.

Top-dress fertilizations with urea were performed, and sprays were applied to control pests and diseases in the crop area. In order to evaluate the green biomass of the crop during different dates, 31 points spaced at 50 m apart were distributed in an area of approximately 7 ha with an irrigated pivot, and the georeferencing of each point was performed with a GPSMAP 60 CSX Garmin® device, as shown in Figure 1.

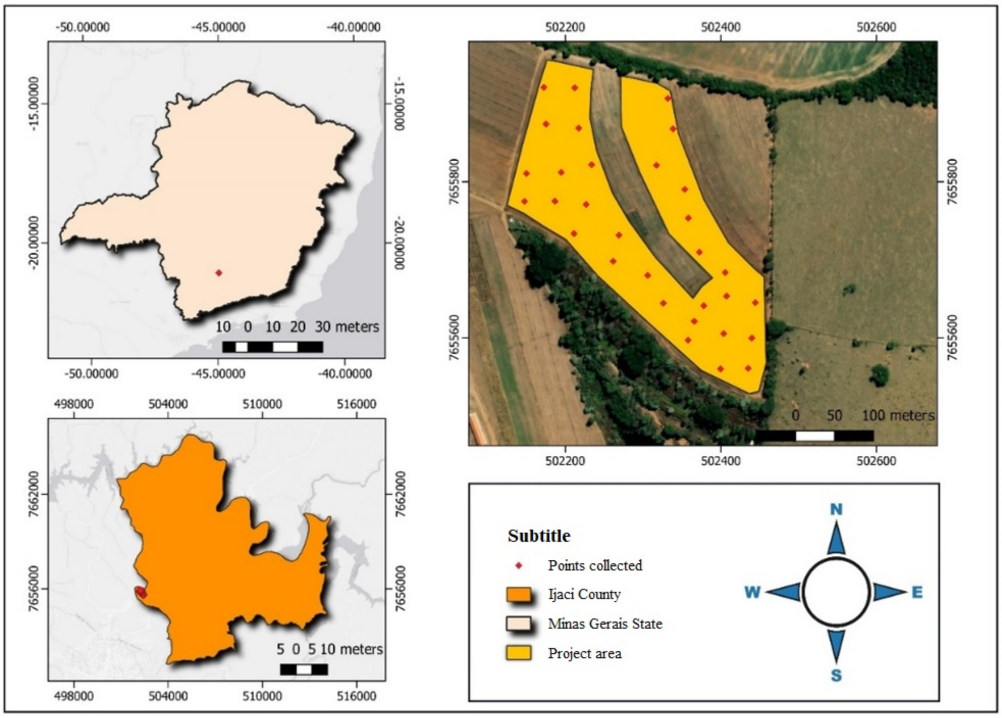

Figure 1. Study location map.

2.1. Green Biomass, Plant Height and Plant Width

Six collections were made during the crop development cycle, starting 15 Days After Sowing (DAS) at the V4 phenological stages of the crop, and at 27, 36, 58, 62 and 76 DAS. For the green biomass evaluation, 0.5 × 0.5 m frames were used to collect plants near georeferenced points.

Subsequently, plants were placed in identified bags, taken to the agriculture department of UFLA for biomass weighting and then inserted into a forced-air circulation oven for 72 h or until reaching constant mass at 65 °C temperature.

Using a graduated tape measure, measurements were taken on three plants from each sampling point. Plant height was measured from the base of the plant to the last fully expanded leaf. For plant width, the distance was measured between the leaves at opposite ends of the plant.

2.2. Satellite Images

The satellite used to collect spectral images was the PlanetScope CubeSat, consisting of 180 nanosatellites (0.10 × 0.10 × 0.30 m) weighing approximately 4 kg each. CubeSat has a one-day temporal resolution, 3 m spatial resolution and a spectral resolution obtained by the PSB.SD sensor with eight bands (Table A1). PlanetScope products have surface reflectance corrections, minimizing the effects caused by the atmosphere. The image correction is performed using correction models such as 6SV2.1 [18], which corrects the top of the atmosphere (TOA) to the bottom of the atmosphere (BOA). However, values are provided as GeoTIFF files on a 10,000 scale, requiring division by this value to obtain reflectance values between 0 and 1. Images were acquired according to the days when plant characteristics were evaluated in the field. When downloading the images a range of 2 days was used to obtain the images near to the collection dates in the field. All used images (five images) were downloaded without cloud cover (0%) in the fields.

2.3. Vegetation Indices

For the estimation of plant green biomass, two vegetation indices were calculated, the Normalized Difference Vegetation Index (NDVI) [19] (Equation (1)), which uses the near-infrared (NIR) and red (RED) bands, and the Normalized Difference Red Edge (NDRE) [20] (Equation (2)), using the wavelengths of *NIR* and red edge.

The chosen vegetation indices relate to crop biomass, such as in the estimation of cynodont grass biomass [21], maize [22], and soybean breeding [23]. The red range is related to chlorophyll, and the infrared range is related to water content in mesophyll cells of the leaves. Therefore, the lower the reflectance in the red range, and the higher reflectance in the *NIR* range, the lower the stresses that the plants are undergoing.

$$NDVI = \frac{NIR - RED}{NIR + RED} \tag{1}$$

where *NDVI*: Normalized Difference Vegetation Index; *NIR*: Near-Infrared; *RED*: red.

$$NDRE = \frac{NIR - RED\ EDGE}{NIR + RED\ EDGE} \tag{2}$$

where *NDRE:* Normalized Difference of Red-Edge; *NIR*: Near Infrared.

The vegetation index calculations were performed within the QGIS 3.26.1 free software, using the raster calculator tool for band combination and index calculation. The extraction of vegetation index values occurred by creating a Voronoi polygon in each point (31) in sequence, and the Voronoi polygon layer was inserted in the tool buffer to create a negative buffer of 2 m to avoid overlapping areas. In total, for each sample point, 31 voronoi polygons with negative buffers were obtained. With the Voronoi polygons and negative buffers created, the zonal statistics tool was used to extract the reflectance values of the vegetation indices. The zonal statistic is a tool in the toolbox of QGIS that is used with input from the Voronoi polygon created with the negative buffer and by extracting the vegetation index (*NDVI* or *NDRE*). The Voronoi polygon informs of the pixels that should be extracted by the zonal statistics tool in the layer vegetation index (*NDVI* or *NDRE*). Using the Voronoi polygons, the tool calculates the maximum, minimum, sum and mean values provided by the vegetation index layer. However, to create the models the value used was the mean obtained in each sample point.

2.4. Multiple Linear Regression Analyses

The data (n = 186) were initially subjected to descriptive analysis: maximum and minimum values, variance, coefficient of variation, standard deviation, and mean, to visualize the behavior of the data and identify possible outliers. In addition, the parameters of width, heigh, *NDVI*, *NDRE*, and green biomass were analyzed by Pearson correlation, selecting those with the best statistical significance ($p < 0.05$) and highest correlation values above 0.6.

After performing the correlation analysis, the data were subjected to multiple linear regression analysis. Multiple linear regression is a technique for approximating functions, with more than one input in the model as an independent variable, and accounting for random errors, which are possible variations that occur outside of the inserted variables [24] (Equation (3)). In this case, fresh biomass values were used as the dependent variable, and the width, height, *NDVI* and *NDRE* parameters were used as independent variables.

To create the models, first, each parameter of the input was select according to the configuration of the models presented in Table 1. After selecting all parameters (axis X) and the green biomass values (axis Y) in the Excel software, the multiple linear regression analysis and the estimated values were obtained. The analysis was divided into two parts, a first analysis with all data (15, 27, 36, 58, 62 and 76) and a second analysis the data of 15, 27 and 36 DAS, representing the time frame in which the plants have not yet completely closed the canopy. At the end of the analysis, the graph was plotted in terms of green biomass estimated (X) and green biomass observed (Y) in the field. The values of R^2 and R were obtained through multiple linear regression analysis and RMSE was calculate afterwards.

$$Y = \beta 0 + \beta 1X1 + \beta 2X2 + \beta 3X3 + \ldots \beta nXn + \varepsilon. \tag{3}$$

where Y represents the estimated value of fresh biomass; $X1$, $X2$, $X3$ and Xn represent independent variables; $\beta1$, $\beta2$, $\beta3$, $\beta4$ and βn are the regression coefficients that will be estimated; and ε is the assumed random error with a normal distribution with mean zero and variance. The evaluation of the models occurred through the values of the coefficient of determination (R^2) (Equation (4)), correlation coefficient (r) (Equation (5)) and root mean square error (RMSE) (Equation (6)).

$$R^2 = \frac{\sum_{i=l}^{N}(Yest_i - \underline{Y})^2}{(Yobs_i - \underline{Y})^2} \tag{4}$$

where *Yest* is the estimated value and *Yobs* is the.

$$R = \frac{\sum_{i=l}^{n}(x_i - \underline{x})\left(y_i - \underline{y}\right)}{\sqrt{[\sum_{i=l}^{n}(x_i - \underline{x})^2(y_i - \underline{y})^2}} \tag{5}$$

where R is the correlation coefficient, x_i and y_i are the values of the variables x and y, and $\underline{x}$ and $\underline{y}$ are the mean values of the variables X and Y.

$$RMSE = \sqrt{\frac{\sum_{i=1}^{n}(y_{obs} - y_{est})^2}{n}} \tag{6}$$

where $RMSE$ is the root mean square error, y_{obs} is the observed value, y_{est} is the value estimated by the model and n is the amount of data. The analysis was carried out using Statistica 7 software, together with Excel software, using the data analysis tool, making it possible to plot graphs and analyze data (Figure 2).

Table 1. Variable correlation of green biomass and bean crops.

Variable	By Variable	Correlation ()	Significance
Green biomass	Height (cm)	0.7230	<0.001
Green biomass	Width (cm)	0.7184	<0.001
Green biomass	*NDVI*	0.7035	<0.001
Green biomass	*NDRE*	0.6155	<0.001

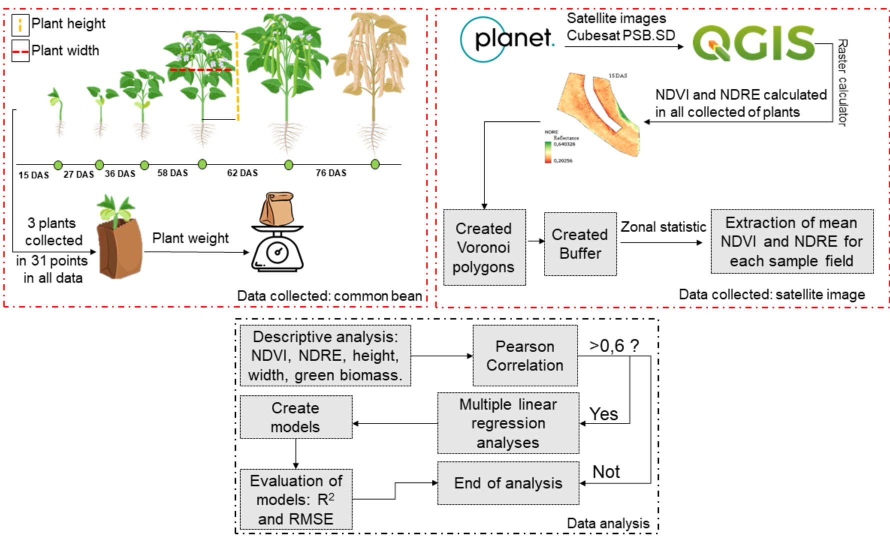

Figure 2. Summary of data collected and data analysis.

3. Results and Discussion

The results of the descriptive measures for all variables are presented in Table A2, where a marked difference between coefficients of variation can be observed. The dataset of biometric parameters, as well as the independent variables, presents a wide range, justified by the sampling distributed throughout the crop development cycle. The common bean plant initially accumulated biomass slowly, with significant potential occurring around 70 DAE [25].

The growth of the stem, lateral branch emission and new leaf production promote biomass accumulation in the plant during the vegetative development stage, persisting throughout the reproductive phase in late-cycle cultivars. In the earlier cultivars, after stage R5, the increase in dry matter occurs mainly due to the production of pods and grains [26]. Plant height and leaf width can be cited as linear measurements that provide information on plant development and are used to estimate biomass.

The variability of reflectance indicated by vegetation indices can be attributed to the dynamics of the crop's phenological stages, due to the increase in leaf area with vegetative and reproductive development of the crop. This finding was also reported by [3], with higher reflectance values detected from 50 DAE onwards. This is similar the results of [27], who demonstrated that biomass can be estimated in a non-destructive and low-cost manner using orbital images. The correlation between the explanatory variables is given in Table 1.

A strong correlation between two variables can be considered when the correlation index values are between 0.7 and 1.0, according to [28]. Thus, it can be observed that the correlations between all variables are high and positive, meaning that there is a high degree of correlation between the explanatory variables.

Green biomass was significantly correlated with plant height and width variables, with correlation coefficients of r = 0.723 and r = 0.718, respectively, as they are related to plant development. The correlation was also significant for the *NDVI* and *NDRE* indices, with the *NDVI* presenting the best correlation coefficient (r = 0.704) and the *NDRE* with lowest value (r = 0.616).

The two vegetation indices (*NDVI* and *NDRE*) are described to be used to measure the biomass of plants. The *NDVI* uses the infrared band in the equation and the *NDRE* uses the red-edge in the equation. The region of responses to chlorophyll and carotenoids is relevant for the study of morphological parameters of the plant, present in wavelengths from 600 to 720 nm, while in the vicinity of 700 to 885 nm is an interesting region for the assessment of green biomass in various crops [29]. This difference in the bands can be related with the sensitivity of the indices in measuring the growth and biomass of the common bean plants.

Therefore, the reflectance response observed within the red edge region and infrared wavelengths have been successfully applied in many researches, such as for the prediction of biomass and leaf nitrogen content in sugarcane [30], high-yield biomass estimation using multispectral imaging in rice [31] and in maize [32], the prediction of dry biomass in strawberry [33] and the estimation of bean production and biomass based on RGB images [34]. *NDVI* has a major sensitivity to *NDRE* due to the plant growth and increase in biomass, which is observed in the Pearson correlation in the Table 1. Due to the sensitivity of this index, good models to predict the yield, estimated chlorophyll *a*, *b* and *total*, and biomass of the other crops with spring wheat can be built with high accuracy and precision [35–37].

Four multiple linear regression models were selected. The green biomass variable was used as a dependent variable in all models. Model 1 (M1) was based on the variables height, width, and *NDVI*. Height, width, and *NDRE* were used in Model 2 (M2), *NDVI* and *NDRE* were used in Model 3 (M3) and height and width in Model 4 (M4).

As shown in Table 2, there was a proximity between all models, with correlation coefficients ranging from 0.73 to 0.75 and R^2 ranging from 0.53 to 0.56. The lowest coefficient of determination was observed in M3, which had a higher RMSE (=5.82) but was still classified as excellent, at lower than 10% [38].

Table 2. Values of the coefficient of determination (R^2), correlation (r) and standard error for the multiple linear regression models.

Models	Coefficient of Correlation (r)	Coefficient of Determination (R^2)	Standard Error	RMSE
M1	0.75	0.56	165.37	1.38
M2	0.74	0.54	168.73	1.33
M3	0.73	0.53	170.38	5.82
M4	0.74	0.54	168.27	2.63
M1 *	0.96	0.93	25.16	24.58
M2 *	0.96	0.92	25.43	24.85
M3 *	0.90	0.81	40.61	39.95
M4 *	0.96	0.92	25.91	25.48

* Models calculated for n = 93 at 15, 27 and 36 days after sowing.

The lowest values observed in M3 can be related to the spatial resolution of the satellite and the number of model parameters. Planet Scope satellites have a spatial resolution of 3 × 3 m, so the variation of biomass must be bigger than that for the satellite capture. When the number of model parameters increases, the models show an improvement, which is observed in M1 and M2.

Figures 3 and 4 show the relationships between observed biomass and biomass estimated from selected models. It can be observed that there is a large dispersion of points around the fitted model in all models (Figure 3) and a small dispersion of points in Figure 4, where the data of R^2 and RMSE are the best. The coefficient of determination (R^2) obtained the best results for the model when comparing the values of plant height and width, demonstrating the potential to combine both biometric variables of the crop. The other multiple linear regression models presented values very close to M1, with M2 and M4 having the same R^2 values and M3 having the lowest value, resulting in a higher error as well (Table 3), except for the data before the plants closed the canopy, where the precision (R^2) was improved and accuracy (RMSE) was decreased.

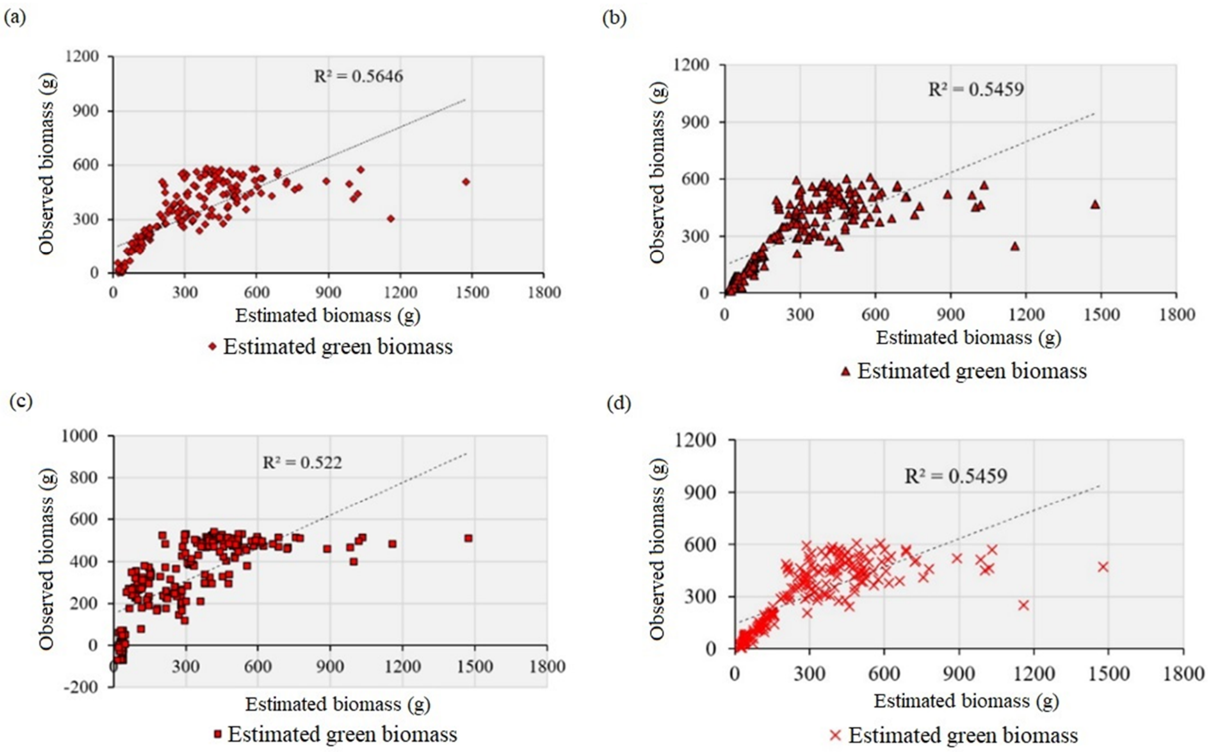

Figure 3. Values obtained by models M1 (**a**), M2 (**b**), M3 (**c**) and M4 (**d**).

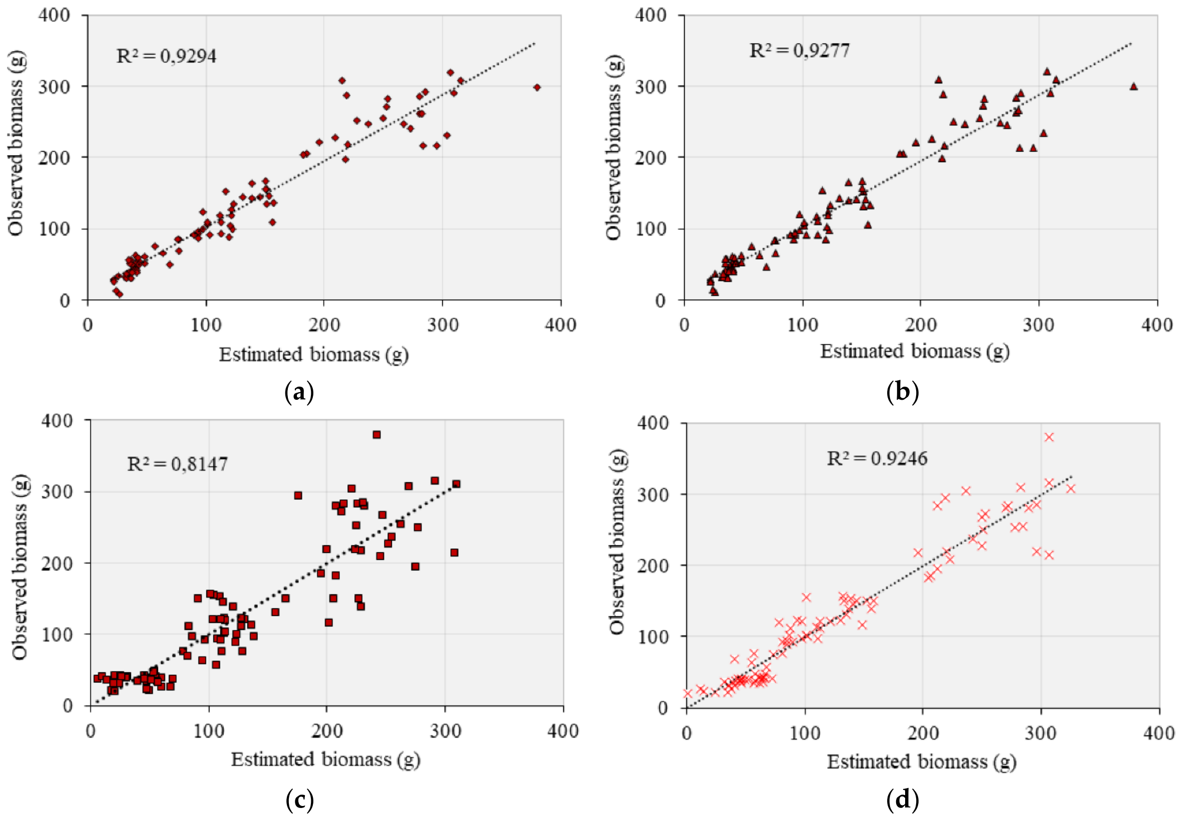

Figure 4. Values obtained by models M1 (**a**), M2 (**b**), M3 (**c**) and M4 (**d**), when the data were analyzed at 15, 27 and 36 days after sowing.

Table 3. Parameters used for estimating green biomass and their respective values.

	Combinations	Coefficients	Standard Error	*p*-Value
M4	Intersection	−187.7240	48.1623	0.0001
	Height (cm)	6.0684	1.7652	0.0007
	Width (cm)	6.8111	2.2474	0.0028
M3	Intersection	−533.6658	62.7488	0.0000
	NDVI	2023.9552	273.3690	0.0000
	NDRE	−11,198.3932	372.1840	0.0015
M2	Intersection	−188.0222	68.8877	0.0070
	Height (cm)	6.0654	1.8376	0.0012
	Width (cm)	6.8059	2.4114	0.0053
	NDRE	1.2650	208.4227	0.9952
M1	Intersection	−339.2907	72.9043	0.0000
	Height (cm)	4.8573	1.7904	0.0073
	Width (cm)	3.8309	2.4631	0.1216
	NDVI	450.1601	164.6879	0.0069
M4 *	Intersection	−91.9320	11.6563	0.0000
	Height (cm)	4.7469	0.5348	0.0000
	Width (cm)	3.3760	0.6529	0.0000
M3 *	Intersection	−234.003	22.6591	0.0000
	NDVI	−709.5394	123.8172	0.0000
	NDRE	1830.1530	164.3382	0.0000

Table 3. *Cont.*

	Combinations	Coefficients	Standard Error	*p*-Value
M2 *	Intersection	−121.931	18.3248	0.0000
	Height (cm)	4.3558	0.5571	0.00005
	Width (cm)	2.8478	0.6887	0.0000
	NDRE	130.1802	62.1121	0.0000
M1 *	Intersection	−119.713	15.7407	0.0000
	Height (cm)	4.7993	0.5197	0.0000
	Width (cm)	2.5261	0.7169	0.0000
	NDVI	89.8283	35.3702	0.0000

* Models calculated for n = 93 at 15, 27 and 36 days after sowing.

The NDVI formula includes spectral bands of near-infrared and red. The red band, ranging from 690 to 720 nanometers, is the range that predominates the absorption by chlorophyll, while good relationships are found in the near-infrared wavelengths ranging from 760 to 800 nanometers, indicating high reflectance [35]. In beans, a reflectance peak starts near 490 nanometers and increases until 550 nanometers, then drops sharply and records lower reflectance between 665 and 680 nanometers [39].

The spectral band provided by satellites and used in the calculation of the *NDVI* vegetation index captures a range of 650 to 680 nanometers, coinciding with the range of greater absorption by chlorophyll and consequently with low reflectance in the range, indicating that the plant is carrying out photosynthesis and increasing its biomass. Conversely, higher reflectance would be observed in this range if the plant is experiencing biotic or abiotic stress. The *NDRE*, another vegetation index used, differs from the *NDVI* in terms of the red-edge range used in its calculation. The band provided by satellites varies from 697 to 713 nanometers, moving away from the range of 665 to 680 nanometers [40], which shows greater detection of chlorophyll, which is reflected in the adjustment of the models.

When comparing the two vegetation indices, the created models showed negative values, with higher RMSE and lower R^2 values. Both vegetation indices were correlated with biomass and sensitive to soil; however, in the early stages of the crop, low reflectance values were found, which for the soil can vary from 0.08 to 0.16 nanometers [41]. Thus, the low values of vegetation indices resulting from the initial growth of plants and low soil coverage negatively affected the estimated values by the model. Similar results were seen by [42] in the initial stages, then observing senescence in the more advanced stages. The authors of [43] reported that depending on the viewing angle and capture time of images, as well as vegetation cover below 22%, vegetation index values were affected by the soil type of the area, ranging from 0.29 to 0.42.

In Figure 5, the values of the normalized difference vegetation index and red-edge normalized difference vegetation index are presented. It is possible to observe that as the days after sowing passed, the vegetation index values increased, demonstrating the increase in green biomass of the crop. Near 62 Days After Sowing (DAS), the highest values of the vegetation indices were found, and from then on, there was a decrease in values, showing the plant senescence process and subsequent harvest.

The *NDVI* values ranged from 0.28 to 0.91, with a sharp increase after the transition between the vegetative and reproductive phases, corresponding to high photosynthetic activity. Similar results were found by [44], where the highest indices were related to the highest yields in bean crops. NDVI is a widely used index for analyzing vegetation cover that is employed in agricultural crops for monitoring the vegetable cycle [45], crop classification [46], and crop yield prediction [47].

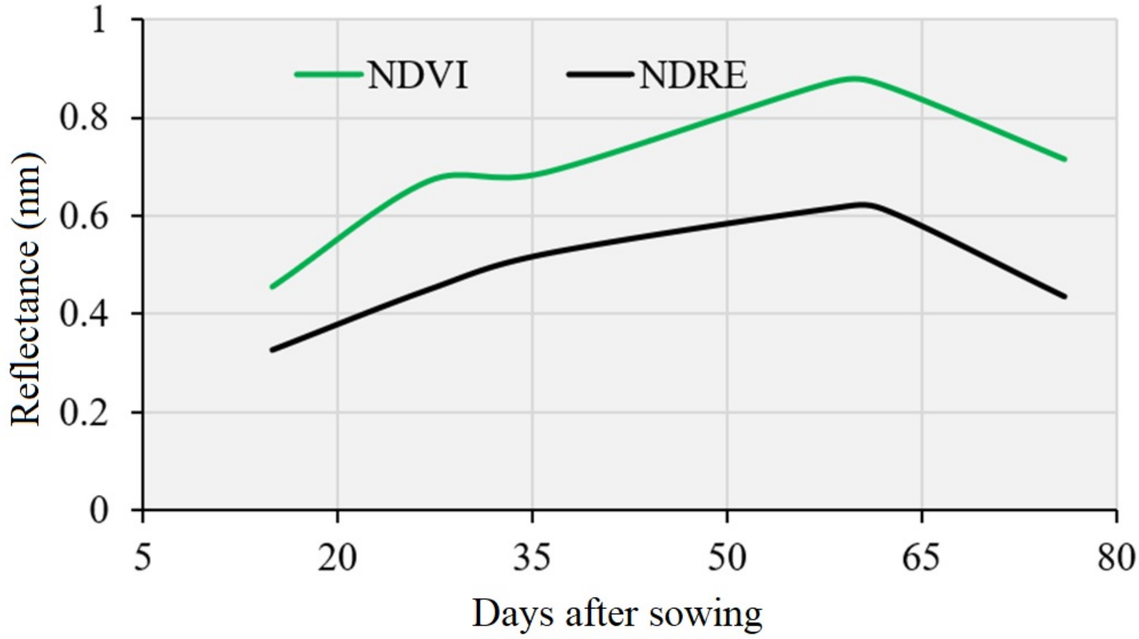

Figure 5. The behavior of vegetation indices and biomass in relation to days after sowing.

The highest *NDVI* value was 0.91, observed at around 62 Days After Sowing (DAS). At this stage of development, the plant concentrates resources on pod emission and beginning of grain filling. Until this stage, NDVI increased throughout the cycle. After the peak, the values decreased due to crop senescence, returning to values similar to those found in the initial phase. Ref. [48] reported similar results, with a peak *NDVI* of 0.80 (R^2 = 0.959) occurring at the R7 stage, demonstrating the potential of the index for monitoring the phenological phases of beans.

The NDRE values varied from 0.19 to 0.69, with a reflectance pattern similar to that observed in the NDVI index throughout the cycle. The lowest NDRE value can be attributed to the reflectance of the RE band, which is less sensitive to chlorophyll content under the canopy [4]. The highest values for the index were also observed at around 62 DAS. Figure 6 shows the dynamics of vegetation indices over the course of crop growth and development, notably presenting at 62 DAS the highest reflectance values for both vegetation indices and demonstrating the highest green tone in the graphs.

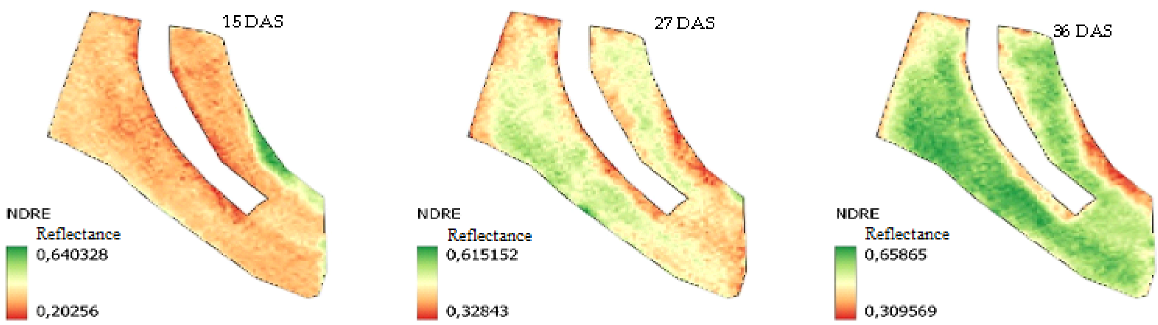

Figure 6. *Cont*.

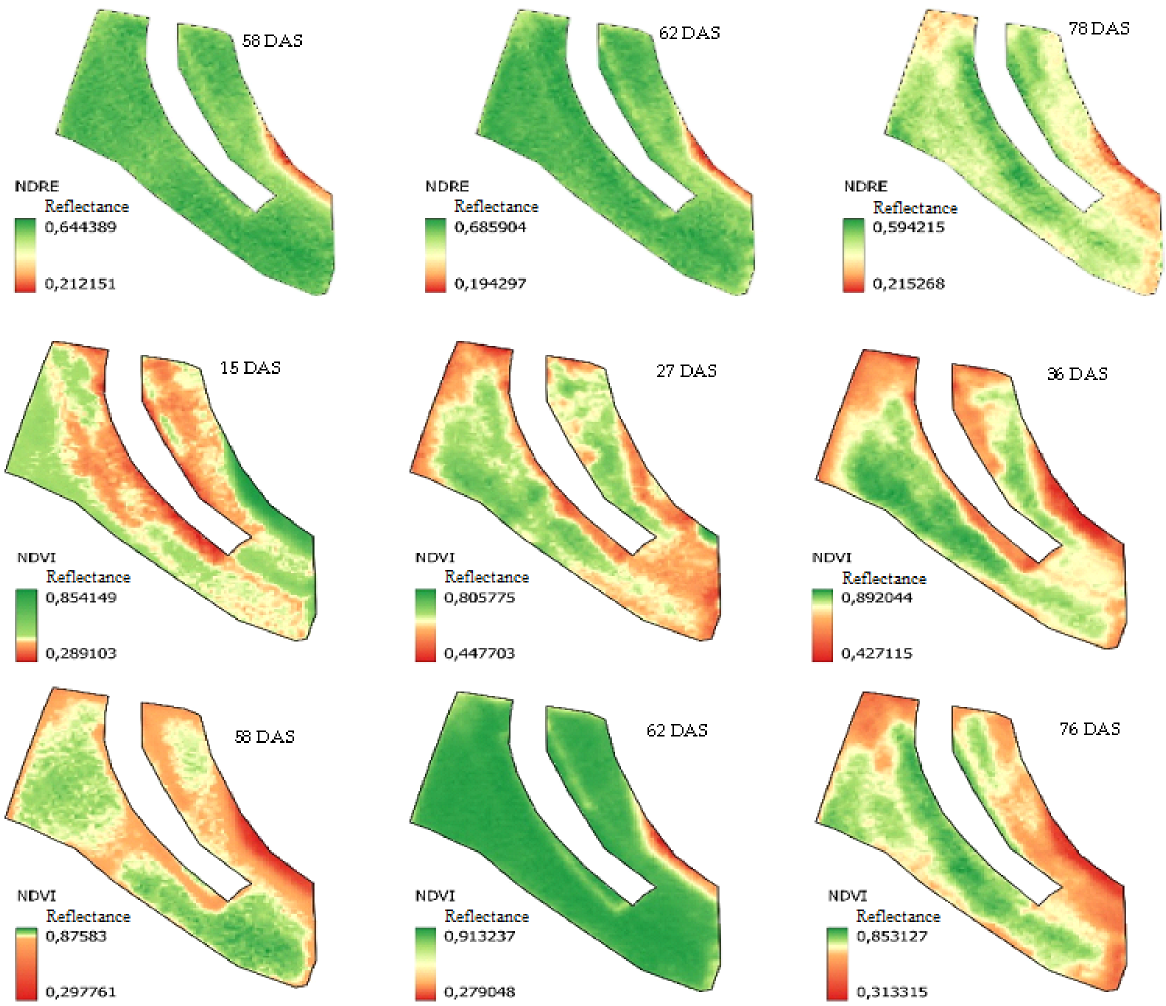

Figure 6. Temporal analysis of common bean using vegetation indices.

The biomass values rapidly increased from 30 to 60 DAS, reaching a peak at 60 DAS, similar to the vegetation indices. The highest leaf area index of the bean crop was observed at around 55 DAS, attributed to the R6 phenological stage, which is the flowering stage of the crop, resulting in low reflectance in the red band and high reflectance in the near-infrared band. At this stage, the plants reach their maximum height [42].

However, this increase in biomass is not always detected by vegetation indices, especially the NDVI, due to saturation [43]. According to [49], saturation values of NDVI are found around 53 to 55 days after emergence or R6 stage of common bean, with maximum index values of 0.83. Therefore, during this reproductive phase, with high leaf area and biomass of the crop, little variation is captured by the vegetation index, indicating that the vegetative phase is the best phase to evaluate the biomass and leaf area of the bean crop [3]. Saturation is also observed in other crops, resulting from low variation in the red band [50].

This changed in the study by [34], in which the estimate of bean biomass obtained relatively stable performance in three growth stages of the crop, namely in the mid bean-filling stage, followed by the podding stage and then the early bean-filling stage. Thus, there was a low variation in the index values between 55 and 62 DAS, with maximum NDVI values of 0.91 and mean values of 0.71, similar to these found by [3,49,51–54].

4. Conclusions

This study was able to understand that vegetation indices (*NDVI* and *NDRE*) are related to the increased biomass of common beans. The models (M1, M2, M3 and M4) showed similar results of accuracy and precision, but Model M1 was the best in terms of precision (R^2 = 0.56) and Model M2 was the best in terms of accuracy (RMSE = 1.33), when analyzed during the bean cycle. For the 15, 27 and 36 DAS models M1 (R^2 = 0.93), M2 (R^2 = 0.92) and M4 (R^2 = 0.92) showed better performance in predicting green biomass when analyzed in the initial stage of culture development, and RMSE values of 24.58, 24.85 and 25.48 g, respectively.

The model that presented the best estimated values for fresh biomass used multiple linear regression analysis with three input parameters: plant width, height, and the vegetation index, *NDVI* or *NDRE*. Despite suffering from saturation starting in the reproductive stages, *NDVI* was better at estimating fresh biomass compared to *NDRE*.

However, when only the values of the vegetation indices were used as input, the models showed lower accuracy and precision, demonstrating that the association with biophysical parameters is important for model calibration. The use of models with only a vegetation index is a method to quantify the biomass and improve the management of crops while only using satellite images. Additionally, this study provided an approach to agricultural management and decision making in precision agriculture.

In this research, two vegetation indices were used to estimate the biomass of common bean plants. In the literature, it is possible to find works that used other vegetation indices and machine learning to estimate biomass, obtaining better model adjustments and superior results. Furthermore, images of other satellites, such as Sentinel and Landsat, can be applied to quantify plant biomass. More studies need to be carried out to test machine learning models with different common bean datasets and other vegetation indices to improve estimation ability.

Author Contributions: Conceptualization, T.O.C.B., M.A.J.F. and A.F.d.S.; methodology, T.O.C.B., M.A.J.F. and A.F.d.S.; software, T.O.C.B.; validation, T.O.C.B. and A.F.d.S.; formal analysis, T.O.C.B., M.A.J.F. and A.F.d.S.; investigation, T.O.C.B., A.F.d.S., G.F.C.S. and M.A.; resources, A.F.d.S.; data curation, T.O.C.B., M.A.J.F. and A.F.d.S.; writing—original draft preparation, T.O.C.B., M.A.J.F. and J.R.F.G.; writing—review and editing, M.A.J.F., T.O.C.B., J.R.F.G. and M.A.; visualization, G.F.C.S., J.R.F.G. and M.A.J.F.; supervision, A.F.d.S.; project administration, A.F.d.S.; funding acquisition, A.F.d.S. All authors have read and agreed to the published version of the manuscript.

Funding: This research received no external funding.

Data Availability Statement: Not applicable.

Acknowledgments: The authors are grateful to the Federal University of Lavras for all its support of this research, and for the Research Support Foundation of the State of Minas Gerais (FAPEMIG) and National Council for Scientific and Technological Development (CNPq) for the students' scholarship. We express our gratitude to Syngenta Digital Brazil for the Imagery platform used for field monitoring.

Conflicts of Interest: The authors declare no conflict of interest.

Appendix A

Table A1. Managing database procedures.

Band	Name	Wave-Length (nm)
1	Coastal blue	431–452
2	Blue	465–515
3	Green I	513–549
4	Green	547–583
5	Yellow	600–620
6	Red	650–680
7	Red-edge	697–713
8	NIR	845–885

Table A2. Descriptive statistics of the independent variables height, width, *NDVI* and *NDRE*, and the dependent variable green biomass.

Parameters	Standard Deviation	Coefficient of Variation	Mean	Minimum	Maximum
Height	16.45	46.34	35.49	8.00	62.00
Width	12.92	30.62	42.20	16.20	64.40
NDVI	0.147	20.64	0.71	0.40	0.90
NDRE	0.107	21.86	0.49	0.29	0.65
Green biomass	248.24	78.78	315.10	20.00	147.50

References

1. De Oliveira, L.F.C.; Oliveira, M.D.C.; Wendland, A.; Heinemann, A.B.; Guimarães, C.M.; Ferreira, E.D.B.; Quintela, E.D.; Barbosa, F.R.; Carvalho, M.D.; Lobo, M., Jr.; et al. Conhecendo a Fenologia do Feijoeiro e Eus Aspectos Fitotécnicos. Brasília: Embrapa. 2018. Available online: https://www.embrapa.br/busca-de-publicacoes/-/publicacao/1085830/conhecendo-a-fenologia-do-feijoeiro-e-seus-aspectos-fitotecnicos (accessed on 1 November 2022).
2. CONAB—Companhia Nacional de Abastecimento. Grãos, Safra 2021/2022. Primeiro Levantamento, Agosto de 2022. Available online: https://www.conab.gov.br/info-agro/safras/graos (accessed on 1 November 2022).
3. De Santana, A.V.; Heinemann, A.B.; Stone, L.F.; Nascente, A.S. Índice de refletância na estimativa da área foliar e biomassa das folhas em feijão-comum. *Colloq. Agrar. Pres. Prudente* **2016**, *12*, 7–19. [CrossRef]
4. Sampaio, M.I.R.; Kunz, A.; Hillebrand, F.L.; Zamberlan, J.F.; Idalino, F.D. Análise dos índices de vegetação NDVI e NDRE em imagens obtidas por meio de sensor embarcado em um RPAS para as culturas da soja (Glycine max) e milho (Zea mays) irrigados. *Rev. Bras. De Geomática* **2021**, *9*, 350–362. [CrossRef]
5. Tsouros, D.C.; Bibi, S.; Sarigiannidis, P.G. A Review on UAV-Based Applications for Precision Agriculture. *Information* **2019**, *10*, 349. [CrossRef]
6. Trentin, C.B.; Trentin, A.B.; Saldanha, D.L. Relação entre a biomassa da vegetação campestre nativa e dados de sensoriamento remoto orbital. *Geographia* **2019**, *21*, 98. [CrossRef]
7. Brandão, Z.N.; Bezerra, M.V.C.; da Silva, B.B. Uso do NDVI para determinação da biomassa na chapada do Araripe. In *Proceedings of the Xiii Simpósio Brasileiro de Sensoriamento Remoto, Florianopolis, Brazil, 21–26 April 2007*; INPE: Florianópolis, Brazil, 2007; pp. 21–26. Available online: http://marte.dpi.inpe.br/col/dpi.inpe.br/sbsr@80/2006/11.15.13.39.22/doc/75-81.pdf (accessed on 22 November 2022).
8. Zhou, X.; Zheng, H.B.; Xu, X.Q.; He, J.Y.; Ge, X.K.; Yao, X.; Cheng, T.; Zhu, Y.; Cao, W.X.; Tian, Y.C. Predicting grain yield in Rice using multi-temporal vegetation índices from UAV based multispectral and digital imagery. *J. Photogramm. Remote Sens.* **2017**, *130*, 246–255. [CrossRef]
9. Debastiani, A.B.; Moura, M.M.; Rex, F.E.; Sanquetta, C.R.; Corte, A.P.D.; Pinto, N. Regressões robusta e linear para estimativa de biomassa via imagem sentinel em uma floresta tropical. *Biofix Sci. J.* **2019**, *4*, 81–87. [CrossRef]
10. Jorge, J.; Vallbé, M.; Soler, J.A. Detection of irrigation in homogeneities in an olive grove using the NDRE vegetation index obtained from UAV images. *Eur. J. Remote Sens.* **2019**, *52*, 169–177. [CrossRef]
11. Trentin, C.; Bredemeier, C.; Vian, A.L.; Drum, M.A.; Santos, F.L. Biomass production and wheat grain yield and its relationship with NDVI as a function of nitrogen availability. *Rev. Bras. De Ciências Agrárias—Braz. J. Agric. Sci.* **2021**, *16*, 1–7. [CrossRef]
12. De Macedo, F.L.; de Oliveira Sousa, A.M.; Gonçalves, A.C.; Silva, H.R.; Rodrigues, R.A.F. Função alométrica de biomassa com imagens de satélite de alta resolução espacial. *Ciência Florest.* **2018**, *28*, 960–969. [CrossRef]
13. Bayaraa, B.; Hirano, A.; Purevtseren, M.; Vandansambuu, B.; Damdin, B.; Natsagdorj, E. Applicability of different vegetation indices for pasture biomass estimation in the north-central region of Mongolia. *Geocarto Int.* **2022**, *37*, 7415–7430. [CrossRef]
14. Carneiro, F.M.; Oliveira, M.F.; Almeida, S.L.H.; Filho, A.L.B.; Furlani, C.E.A.; Rolim, G.S.; Ferraudo, A.S.; Silva, R.P. Biophysical characteristics of soybean estimated by remote sensing associated with artificial intelligence. *Biosci. J.* **2022**, *38*, 1981–3163. [CrossRef]
15. Venancio, L.P.; Mantovani, E.C.; Amaral, C.H.; Neale, C.M.U.; Gonçalves, I.Z.; Filgueiras, R.; Eugenio, F.C. Potential of using spectral vegetation indices for corn green biomass estimation based on their relationship with the photosynthetic vegetation sub-pixel fraction. *Agric. Water Manag.* **2020**, *236*, 106155. [CrossRef]
16. Köppen, W.; Geiger, R. *Klimate der Erde*; Verlag Justus Perthes: Gotha, Germany, 1928.
17. Dantas, A.A.A.; Carvalho, L.G.; Ferreira, E. Classificação e tendências climáticas em Lavras, MG. *Ciência Agrotec.* **2007**, *31*, 1862–1866. [CrossRef]
18. Kotchenova, Y.S.; Vermote, E.F. Validation of a vector version of the 6S radiative transfer code for atmospheric correction of satellite data. Part II. Homogeneous Lambertian and anisotropic surfaces. *Appl. Opt.* **2007**, *46*, 4455–4464. [CrossRef]
19. Rouse, J.W. *Monitoring the Vernal Advancement and Retrogradation of Natural Vegetation (Green Wave Effect) of Natural Vegetation*; Texas A&M University: College Station, TX, USA; National Aeronautics and Space Administration: Washington, DC, USA, 1974; p. 371.

20. Sims, D.A.; Gamon, J.A. Relationships between leaf pigment content and spectral reflectance across a wide range of species, leaf structures and developmental stages. *Remote Sens. Environ.* **2002**, *81*, 337–354. [CrossRef]
21. Hott, M.C.; Andrade, R.G.; de Magalhaes, W.C.P., Jr.; Benites, F.R.G. Uso de veículo aéreo não tripulado (VANT) para estimativa de vigor e de correlações agronômicas em genótipos de capim cynodon. In *Engenharia Sanitária e Ambiental*; Atena Editora: Ponta Grossa, Brazil, 2018; Volume Chapter 22, pp. 235–244. Available online: https://www.infoteca.cnptia.embrapa.br/handle/doc/1119158 (accessed on 10 December 2022).
22. Zhang, Y.; Xia, C.; Zhang, X.; Cheng, X.; Feng, G.; Wang, Y.; Gao, Q. Estimating the maize biomass by crop height and narrowband vegetation índices derived from UAV-based hyperespectral images. *Ecol. Indic.* **2021**, *129*, 107985. [CrossRef]
23. Sakurai, K.; Toda, Y.; Kajiya-Kanegae, H.; Ohmori, Y.; Yamasaki, Y.; Takahashi, H.; Takanashi, H.; Tsuda, M.; Tsujimoto, H.; Kaga, A.; et al. Time-series multi-spectral imaging in soybean for improving biomass and genomic prediction accuracy. *bioRxiv* **2021**. [CrossRef]
24. Workman, J., Jr.; Burns, D.A.; Ciurczak, E.W. (Eds.) *Handbook of Near-Infrared Analysis*; Marcel Dekker, Inc.: New York, NY, USA, 1992; pp. 274–276.
25. Pegoraro, R.F.; Oliveira, D.; Moreira, C.G.; Kongo, M.K.; Portugal, A.F. Partição de biomassa e absorção de nutrientes pelo feijoeiro comum. *Rev. Caatinga* **2014**, *27*, 41–52.
26. Gomes, A.A.; Araújo, A.P.; Rossielo, R.O.P.; Pimentel, C. Acumulação de biomassa, características fisiológicas e rendimento de grãos em cultivares de feijoeiro irrigado e sob sequeiro. *Pesqui. Agropecuária Bras.* **2000**, *35*, 1927–1937. [CrossRef]
27. Andrade, C.A.B.; Scapim, C.A.; Braccini, A.L.; Martorelli, D.T. Produtividade, crescimento e partição de matéria seca em duas cultivares de feijão. *Acta Sci. Agron.* **2009**, *31*, 683–688. [CrossRef]
28. Ramos, A.; Bovi, M.L.A.; Folegatti, M.V.; Diotto, A.V. Estimativas da área foliar e da biomassa aérea da pupunheira por meio de relações alométricas. *Hortic. Bras.* **2008**, *26*, 138–143. [CrossRef]
29. Trevisan, L.R.; Brichi, L.; Gomes, T.M.; Rossi, F. Estimating Black Oat Biomass Using Digital Surface Models and a Vegetation Index Derived from RGB-Based Aerial Images. *Remote Sens.* **2023**, *15*, 1363. [CrossRef]
30. Shendryk, Y.; Sofonia, J.; Garrard, R.; Rist, Y.; Skocaj, D.; Thorburn, P. Fine-scale prediction of biomass and leaf nitrogen content in sugarcane using UAV LiDAR and multispectral imaging. *Int. J. Appl. Earth Obs. Geoinf.* **2020**, *92*, 102177. [CrossRef]
31. Devia, C.A.; Rojas, J.P.; Petro, E.; Martinez, C.; Mondragon, I.F.; Patino, D.; Rebolledo, M.C.; Colorado, J. High-Throughput Biomass Estimation in Rice Crops Using UAV Multispectral Imagery. *J. Intell. Robot. Syst.* **2019**, *96*, 573–589. [CrossRef]
32. Shu, M.; Shen, M.; Dong, Q.; Yang, X.; Li, B.; Ma, Y. Estimating the maize above-ground biomass by constructing the tridimensional concept model based on UAV-based digital and multi-spectral images. *Field Crops Res.* **2022**, *282*, 108491. [CrossRef]
33. Zheng, C.; Abd-Elrahman, A.; Whitaker, V.; Dalid, C. Prediction of Strawberry Dry Biomass from UAV Multispectral Imagery Using Multiple Machine Learning Methods. *Remote Sens.* **2022**, *14*, 4511. [CrossRef]
34. Ji, Y.; Liu, R.; Xiao, Y.; Cui, Y.; Chen, Z.; Zong, X.; Yang, T. Faba bean above-ground biomass and bean yield estimation based on consumer-grade unmanned aerial vehicle RGB images and ensemble learning. *Precis. Agric.* 2023. [CrossRef]
35. Luz, L.R.; Giongo, V.; dos Santos, A.M.; de Carvalho Lopes, R.J.; de Lima, C., Jr. Biomass and vegetation index by remote sensing in different caatinga forest areas. *Ciência Rural.* **2022**, *52*, e20201104. [CrossRef]
36. Dancey, C.; Reidy, J. Estatística sem matemática para psicologia: Usando SPSS para Windows. In *Desvendando os Mistérios do Coeficiente de Correlação de Pearson (r)*; Filho, D.B.F., Júnior, J.A.S., Eds.; Revista Política Hoje: Recife, Brazil, 2009; Volume 18, Available online: https://periodicos.ufpe.br/revistas/politicahoje/article/viewFile/3852/3156Test (accessed on 15 December 2022).
37. Monteiro, P.F.C.; Filho, R.A.; Xavier, A.C.; Monteiro, R.O.C. Índices de vegetação simulados de diferentes sensores na estimativa das variáveis biofísicas do feijoeiro. *Pesqui. Agropecuária Bras.* **2013**, *48*, 433–441. [CrossRef]
38. Qiao, L.; Tang, W.; Gao, D.; Zhao, R.; An, L.; Li, M.; Sun, H.; Song, D. UAV-based chlorophyll content by evaluating vegetation index responses under different crop coverages. *Comput. Electron. Agric.* **2022**, *196*, 106775. [CrossRef]
39. Atkinson Amorim, J.G.; Schreiber, L.V.; de Souza, M.R.Q.; Negreiros, M.; Susin, A.; Bredemeier, C.; Trentin, C.; Vian, A.L.; de Oliveira Andrades-Filho, C.; Doering, D.; et al. Biomass estimation of spring wheat with machine learning methods using UAV-based multispectral imaging. *Int. J. Remote Sens.* **2022**, *43*, 4758–4773. [CrossRef]
40. Jamieson, P.D.; Porter, J.R.; Wilson, D.R. A test of the computer simulation model ARCWHEAT 1 on wheat crops grown in New Zealand. *Field Crops Res.* **1991**, *27*, 337–350. [CrossRef]
41. Gitelson, A.A.; Keydan, G.P.; Merzlyak, M.N. Three-band model for noninvasive estimation of chlorophyll, carotenoids, and anthocyanin contents in higher plant leaves. *Geophys. Res. Lett.* **2006**, 33. [CrossRef]
42. Yu, D.; Lord, N.; Polk, J.; Dhakal, K.; Li, S.; Yin, Y.; Duncan, S.E.; Wang, H.; Zhang, B.; Huang, H. Physical and chemical properties of edamame during bean development and application of spectroscopy-based machine learning methods to predict optimal harvest time. *Food Chem.* **2022**, *368*, 130799. [CrossRef] [PubMed]
43. Nagler, P.L.; Daughtry, C.S.T.; Goward, S.N. Planta litter and soil reflectance. *Remote Sens. Environ.* **2000**, *71*, 207–215. [CrossRef]
44. Monteiro, P.F.C.; Filho, R.A.; Xavier, A.C.; Monteiro, R.O.C. Assessing biophysical variable parameters of bean crop with hyperspectral measurements. *Sci. Agric.* **2012**, *69*, 87–94. [CrossRef]
45. Epiphano, J.C.N.; Gleriani, J.M.; Formaggio, A.R.; Rudorff, B.F.T. Índices de vegetação no sensoriamento remoto da cultura do feijão. *Pesqui. Agropecuária Bras.* **1996**, *31*, 445–454.

46. Filho, R.A.; Cunha, C.A.H.; Rudorff, B.F.T.; Moreira, A.M. Comportamento Espectral da Cultura do Feijão (IAC—Carioca 80) Irrigado com Diferentes Lâminas de Água. Anais X SBSR, Foz do Iguaçu, INPE, p. 3–10. 2001. Available online: http://marte.sid.inpe.br/col/dpi.inpe.br/lise/2001/09.12.16.28/doc/0003.10.007.pdf (accessed on 20 December 2022).
47. Venancio, L.P.; Filgueiras, R.; Cunha, F.F.; Silva, F.C.S.; Santos, R.A.; Mantovani, E.C. Mapeamento dos estádios fenológicos da cultura do milho utilizando o NDVI derivado dos sensores OLI e MODIS. *Semin. Ciências Agrárias* **2020**, *41*, 1517–1534. [CrossRef]
48. Coelho, A.H.R.; Franco, A.H.B.M.; Franco, W.S.; Anjos, C.S. Caracterização dos Estádios Fenológicos da Soja no Município de Sorriso-MT Utilizando NDVI e Classificação de Imagens não Supervisionada. Anais [...], Santos, INPE, p. 1116–1119. 2019. Available online: https://proceedings.science/sbsr-2019/papers/caracterizacao-dos-estadios-fenologivos-da-soja-no-municipio-de-sorriso-mt-utilizando-ndvi-e-classificacao-de-imagens-na?lang=pt-br (accessed on 10 January 2023).
49. Pontes, P.P.B.; Rocha, J.V.; Lamparelli, R.A.C. Análise Temporal de Índices de Vegetação como Subsídio à Previsão de Safras de Cana-De-Açúcar. Anais [...], Goiânia, INPE, p. 217–224. 2005. Available online: http://marte.sid.inpe.br/col/ltid.inpe.br/sbsr/2004/11.21.21.12/doc/217.pdf (accessed on 10 January 2023).
50. Silva, G.F.C.; Nanni, M.R.; da Silva, C.A., Jr.; Crusiol, L.G.T.; Furlanetto, R.H.; Facco, C.U.; Campos, T.L.L.; Souza, J.S.; Sacioto, M. Comportamento Espectral dos Diferentes Estágios Fenológicos na Cultura do Feijão. Anais [...], Santos, INPE, p. 6490–6597. 2017. Available online: http://marte2.sid.inpe.br/attachment.cgi/sid.inpe.br/marte2/2017/10.27.15.48.49/doc/60157.pdf (accessed on 17 January 2023).
51. Filla, V.A.; Coelho, A.P.; Bettiol, J.V.T.; Leal, F.T.; Lemos, L.B.; Rosalen, D.L. Model performance in estimating the yield of common bean cultivars. *Rev. Ciência Agronômica* **2023**, *54*. [CrossRef]
52. Tenreiro, T.R.; Vila-García, M.; Gómez, J.A.; Berni-Jirménez, J. Using NDVI for the assesmen of canopy cover in agricultural crops within modelling research. *Comput. Electron. Agric.* **2021**, *182*, 106038. [CrossRef]
53. Prudente, V.H.R.; Mercante, E.; Johann, J.A.; Souza, C.H.W.D.; Cattani, C.E.V.; Mendes, I.S.; Caon, I.L. Use of terrestrial remote sensing to estimate soybeans and beans biophysical parameters. *Geocarto Int.* **2021**, *36*, 773–790. [CrossRef]
54. Sankaran, S.; Quirós, J.J.; Miklas, P.N. Unmanned aerial system and satellite-based high resolution imagery for high-throughput phenotyping in dry bean. *Comput. Electron. Agric.* **2019**, *165*, 104965. [CrossRef]